Theoretical Expression of the Aperture-averaged Irradiance Scintillation Index (ISI) for a Gaussian Beam in Non-Kolmogorov Turbulence with Finite Inner and Outer Scales

C. GAO AND X-F. LI*

School of Astronautics and Aeronautic, University of Electronic Science and Technology of China, 2006 Xiyuan Avenue, West Hi-Tech Zone, Chengdu 611731, Sichuan Province, China

This paper investigates the aperture-averaged irradiance scintillation index of a Gaussian beam propagating through a horizontal path in weak anisotropic turbulence. Analytical expressions are deduced based on the generalized exponential atmospheric spectrum for anisotropic turbulence, which includes the spectral power law value of non-Kolmogorov turbulence, the finite inner and outer scales of turbulence, the anisotropic factor, and other optical parameters of the Gaussian beam. The numerical results indicate that the aperture-averaged irradiance scintillation index (ISI) is more sensitive to the change of the inner scale than the outer scale, and an increasing aperture diameter or an increasing anisotropic factor can decrease the irradiance scintillation index at the receiver.

Keywords: Wireless laser communications, Gaussian beam, anisotropic non-Kolmogorov turbulence, inner and outer scales of turbulence, aperture-averaged effect, irradiance scintillation index (ISI)

1 INTRODUCTION

Wireless laser communication is a type of point-to-point communication technology. It uses unguided laser beam propagating in free space to carry

---

*Corresponding author: E-mail: lxf3203433@uestc.edu.cn

the digital signal for data transmission and information swap [1, 2]. The performance of an optical wireless communication system can be heavily influenced by the atmospheric turbulence effects, which will degenerate the laser's coherence and reduce the carrier's quality. As an atmospheric turbulence effects, the irradiance scintillation can cause the stochastic fluctuation of photocurrents output by the detector in the receiver; thus, to achieve a certain bit error rate, the required signal-to-noise ratio is larger than that in the turbulence-free channel [3-5].

The irradiance scintillation is a physical phenomenon, which implies the fluctuation of the instant luminous power around the average of the incident beam at the receiving antenna given that the power of the outgoing beam is fixed at the transmitting antenna. For theoretical analyses of the irradiance scintillation under different situations, various power spectrum models of refractive index have been proposed in the past few decades. Andrews and Philips [1] summarizes the irradiance scintillation index (ISI) for a Gaussian beam with various Kolmogorov-based models, and other workers [6-13] conducted similar research with various non-Kolmogorov-based models. The aforementioned literature, however, usually divides the ISI into radial (off-axis) and longitudinal (on-axis) components, and thus ignore the aperture-averaged effect. Toselli and Korotkova [14], Cheng *et al.* [15] and Gao *et al* [16] report the ISI with the aperture-averaged effect for a Gaussian beam in weak non-Kolmogorov turbulence. Toselli and Korotkova [14] go further and consider the anisotropy of turbulence, but supposes the outer scale diverges to infinity while inner scale equates to zero. Cheng *et al.* [15] and Gao *et al.* [16] take finite outer scale and positive inner scale into account, but Gao *et al.* [16] fails to give the analytical expressions of their deduced model, whereas Cheng *et al.* [15] presents theoretical expressions with some limitations.

This paper investigates the aperture-averaged ISI for a Gaussian beam propagating in weak anisotropic turbulence along a horizontal path. The mathematical model of this paper also contains the inner and outer scales of turbulence, and the corresponding analytical expressions are deduced by complex analysis. Our work can be regarded as incremental to previous literatures.

2 APERTURE-AVERAGED IRRADIANCE SCINTILLATION INDEX (ISI) FOR A GAUSSIAN BEAM

The Gaussian beam is a representative type of electromagnetic wave, with normally distributed transverse electric field and intensity. The mathematical description of a Gaussian beam usually depends on the wavelength λ and the waist radius w. As for the optical wireless communication, more parameters are necessary to determine the location of both the transmitter and the

receiver. The curvature parameter, Θ_0,

$$\Theta_0 = 1 - \frac{L}{R_0} \tag{1a}$$

and the Fresnel ratio, Λ_0,

$$\Lambda_0 = \frac{2L}{k W_0^2} \tag{1b}$$

are two nondimensional parameters related to the transmitter, where L is the propagation path length, R is the radius of curvature of the phase wavefront at the transmitter, $k = \frac{2\pi}{\lambda}$ is the angular wavenumber, and W is the radius where the intensity reduce to $\frac{1}{e^2}$ of the axial values at the transmitter. Similarly, there are also three nondimensional parameters, the refraction parameter, Θ,

$$\Theta = \frac{\Theta_0}{\Theta_0^2 + \Lambda_0^2} \tag{1c}$$

the complementary parameter, $\bar{\Theta}$,

$$\bar{\Theta} = 1 - \Theta \tag{1d}$$

and the diffraction parameter, Λ

$$\Lambda = \frac{\Lambda_0}{\Theta_0^2 + \Lambda_0^2} \tag{1e}$$

related to the receiver [1].

The aperture-averaged ISI of a Gaussian beam propagating through weak atmospheric turbulence in the absence of beam wander takes the form [14]

$$
\begin{aligned}
\sigma_{ISI}^2 (D_G) \quad = \quad & 8\pi^2 k^2 L \int_0^1 d\xi \int_0^{+\infty} d\kappa \times \kappa \Phi_n (\kappa) \\
& \times \exp\left(-\frac{L\kappa^2}{k(\Omega_G + \Lambda)} \left(\left(1 - \bar{\Theta}\xi\right)^2 + \Lambda \Omega_G \xi^2\right)\right) \\
& \times \left(1 - \cos\left(\frac{L\kappa^2}{k} \left(\frac{\Omega_G - \Lambda}{\Omega_G + \Lambda}\right) \xi \left(1 - \bar{\Theta}\xi\right)\right)\right)
\end{aligned} \tag{2}
$$

where $\xi = 1 - \frac{z}{L}$ is the normalized path coordinate, z is the coordinate along the propagation direction, $\Omega_G = \frac{16L}{kD_G^2} > \Lambda$ is a nondimensional parameter characterizing the relative radius of the collecting lens, D_G is the collecting lens diameter and $\Phi_n (\kappa)$ is the power spectrum of the refractive index.

For mathematical convenience, this paper invokes the exponential spectrum for further discussion. The generalized exponential spectrum for
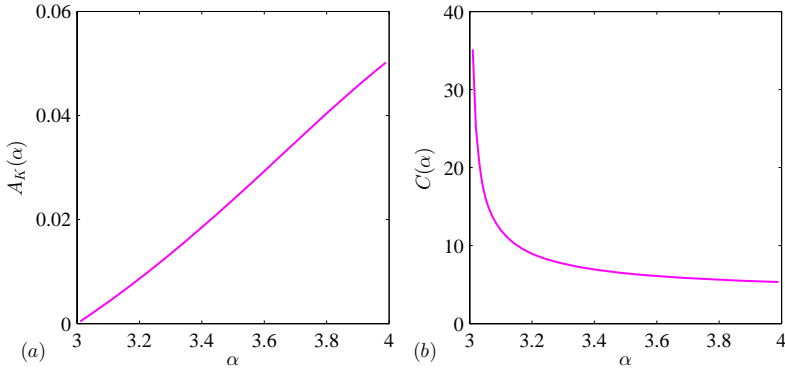
FIGURE 1
Graphs showing (a) $A(\alpha)$ and (b) $C(\alpha)$ as a function of the spectral power law α

anisotropic turbulence takes the form [17]

$$\Phi_n(\kappa) = A(\alpha)\,\hat{C}_n^2 \varsigma_e^{2-\alpha} \kappa^{-\alpha} \left(1 - \exp\left(-\frac{\varsigma_e^2 \kappa^2}{\kappa_L^2}\right)\right) \exp\left(-\frac{\varsigma_e^2 \kappa^2}{\kappa_H^2}\right) \qquad (3)$$

where $\kappa = \sqrt{\kappa_x^2 + \kappa_y^2 + \kappa_z^2}$ is the scalar spatial wavenumber related to the size of the turbulence cell with components κ_x, κ_y, and κ_z in the $x-$, $y-$, and z-directions, respectively. $\alpha \in (3, 4)$ is the general spectral power law value, $A(\alpha) = \frac{\Gamma(\alpha-1)}{4\pi^2} \cos\frac{\alpha\pi}{2}$ is a function related to α. The symbol $\Gamma(\cdot)$ denotes the gamma function. $\kappa_L = \frac{4\pi}{L_0}$ is the low cut-off wavenumber related to the outer scale L_0, whereas $\kappa_H = \frac{C(\alpha)}{l_0}$ is the high cut-off wavenumber related to the inner scale l_0 with $C(\alpha) = \left(\frac{\pi(3-\alpha)}{3} A(\alpha)\, \Gamma\left(\frac{3-\alpha}{2}\right)\right)^{\frac{1}{\alpha-5}}$. $\hat{C}_n^2$ is the generalized atmospheric structure parameter, and ς_e is the anisotropic factor. When ς_e is equal to one, the turbulence becomes isotropic. When ς_e increases, the anisotropic property of turbulence enhances.

Figure 1 depicts $A(\alpha)$ and $C(\alpha)$ as a function of the spectral power law α. It can be seen that $A(\alpha)$ increases monotonically from $\lim\limits_{\alpha\to 3} A(\alpha) = 0$ while $C(\alpha)$ decreases monotonically. Thus, the cut-off wavenumber at high κ_H decreases with an increase in the spectral power law α.

3 EXPRESSION REDUCTION

This section presents the derivation of the closed-form expression of Equation (2). Without loss of generality, we define

$$\begin{cases} P(\xi) = \frac{L}{k(\Omega_G+\Lambda)} \left((1 - \bar{\Theta}\xi)^2 + \Lambda\Omega_G\xi^2\right) \\ Q(\xi) = \frac{L}{k}\left(\frac{\Omega_G-\Lambda}{\Omega_G+\Lambda}\right)\xi\left(1 - \bar{\Theta}\xi\right) \end{cases} \qquad (4)$$

Based on the Euler's formula, we can get [18]

$$(1 - \cos (Q(\xi)\kappa^2)) = \Re (1 - \exp (i Q(\xi)\kappa^2)) \qquad (5)$$

where the $\Re$ means the real part of a complex number, and i stands for the imaginary unit. For the convenience of mathematics, let

$$f(\kappa) = \sum_{j=1}^{2} (-1)^{j-1} \exp\left(-d_j^2 \kappa^2\right) \qquad (6)$$

where $d_1 = \sqrt{\frac{\varsigma_e^2}{\kappa_H^2}}$ and $d_2 = \sqrt{\frac{\varsigma_e^2}{\kappa_L^2} + \frac{\varsigma_e^2}{\kappa_H^2}}$. Now, Equation (3) can be rewritten as

$$\Phi_n(\kappa) = A(\alpha) \hat{C}_n^2 \varsigma_e^{2-\alpha} \kappa^{-\alpha} \times f(\kappa) \qquad (7)$$

Substituting Equations (4), (5) and (7) into Equation (2), it follows that

$$\sigma_{ISI}^2(D_G) = 8\pi^2 k^2 L A(\alpha) C_n^2 \varsigma_e^{2-\alpha} \int_0^1 d\xi \int_0^{+\infty} d\kappa \qquad (8)$$
$$\times \Re \kappa^{1-\alpha} f(\kappa) \left(\exp\left(-P(\xi)\kappa^2\right) - \exp\left(-(P(\xi) + i Q(\xi))\kappa^2\right)\right)$$

To compute the iterated integral in Equation (8), expand the integrand by Equation (6):

$$\Re \kappa^{1-\alpha} f(\kappa) \left(\exp\left(-P(\xi)\kappa^2\right) - \exp\left(-(P(\xi) + i Q(\xi))\kappa^2\right)\right)$$
$$= \Re \kappa^{1-\alpha} \sum_{j=1}^{2} (-1)^{j-1} \left(\exp\left(-\left(P(\xi) + d_j^2\right)\kappa^2\right)\right) \qquad (9)$$
$$- \exp\left(-\left(P(\xi) + d_j^2 + i Q(\xi)\right)\kappa^2\right)$$

Based on the equation for $p > -3$, $\Re u > 0$, and $\Re v > 0$ [19], then

$$\int_0^{+\infty} x^p \left(\exp\left(-ux^2\right) - \exp\left(-vx^2\right)\right) dx$$
$$= \frac{1}{p+1} \left(u^{-\frac{p+1}{2}} - v^{-\frac{p+1}{2}}\right) \Gamma\left(\frac{p+3}{2}\right) \qquad (10)$$

and the double integrals in Equation (7) can be reduced to

$$\int_0^1 d\xi \int_0^{+\infty} \Re \kappa^{1-\alpha} f(\kappa) \left(\exp\left(-P(\xi)\kappa^2\right) - \exp\left(-(P(\xi) + i Q(\xi))\kappa^2\right)\right) d\kappa$$
$$= \Re \frac{1}{2-\alpha} \Gamma\left(\frac{4-\alpha}{2}\right) \sum_{j=1}^{2} (-1)^{j-1} \int_0^1 \left(\left(P(\xi) + d_j^2\right)^{-\frac{2-\alpha}{2}} \qquad (11)$$
$$- \left(P(\xi) + d_j^2 + i Q(\xi)\right)^{-\frac{2-\alpha}{2}}\right) d\xi$$

According to Equation (4), both

$$
\begin{cases}
G_{1,j}(\xi) = P(\xi) + d_j^2 \\
G_{2,j}(\xi) = P(\xi) + iQ(\xi) + d_j^2
\end{cases}
\tag{12}
$$

are univariate quadratic polynomials about ξ; thus, $G_{l,j}(\xi)$ can be factorized in the complex field by

$$
G_{l,j}(\xi) = z_l\left(\xi - r_{l,j}\right)\left(\xi - s_{l,j}\right)
\tag{13}
$$

where $r_{l,j}$ and $s_{l,j}$ are roots of $G_{l,j}(\xi) = 0$, $z_1 = \frac{L(\bar\Theta^2 + \Lambda\Omega_G)}{k(\Omega_G + \Lambda)}$ and $z_2 = z_1 - i\frac{L\bar\Theta(\Omega_G - \Lambda)}{k(\Omega_G + \Lambda)}$. Since $\forall \xi \in \mathrm{R}: P(\xi) > 0$, the imaginary part of both $r_{l,j}$ and $s_{l,j}$ must be nonzero. Let $q = \frac{\alpha-2}{2}$ and $\xi = \eta + \frac{r_{l,j}+s_{l,j}}{2}$, we can get

$$
\int_0^1 \left(G_{l,j}(\xi)\right)^q \, \mathrm{d}\xi = z_{2,l}^q \int_{-\frac{r_{l,j}+s_{l,j}}{2}}^{1-\frac{r_{l,j}+s_{l,j}}{2}} \left(\eta^2 - \left(\frac{r_{l,j}-s_{l,j}}{2}\right)^2\right)^q \mathrm{d}\eta
\tag{14}
$$

When $r_{l,j} = s_{l,j}$, because $\frac{1}{2} < q = \frac{\alpha-2}{2} < 1$, Equation (14) becomes

$$
\int_{-\frac{r_{l,j}+s_{l,j}}{2}}^{1-\frac{r_{l,j}+s_{l,j}}{2}} \eta^{2q}\, \mathrm{d}\eta = \frac{1}{2p+1}\left(\left(1 - \frac{r_{l,j}+s_{l,j}}{2}\right)^{2p+1} - \left(-\frac{r_{l,j}+s_{l,j}}{2}\right)^{2p+1}\right)
\tag{15}
$$

When $r_{l,j} \neq s_{l,j}$, the integrand in Equation (14) is a meromorphic function, whose finite isolated singularities can be removable. So, the integrand in Equation (14) is holomorphically extendable over the complex plane by the analytic continuation [20]. Based on the Cauchy's integral theorem in complex analysis, the value of Equation (14) is independent to the path of integration. For any bounded simple connected convex region containing $-\frac{r_{l,j}+s_{l,j}}{2}$, $1 - \frac{r_{l,j}+s_{l,j}}{2}$ and 0, we can get

$$
\begin{aligned}
&\int_{-\frac{r_{l,j}+s_{l,j}}{2}}^{1-\frac{r_{l,j}+s_{l,j}}{2}} \left(\eta^2 - \left(\frac{r_{l,j}-s_{l,j}}{2}\right)^2\right)^q \mathrm{d}\eta \\
&= \int_0^{1-\frac{r_{l,j}+s_{l,j}}{2}} \left(\eta^2 - \left(\frac{r_{l,j}-s_{l,j}}{2}\right)^2\right)^q \mathrm{d}\eta - \int_0^{-\frac{r_{l,j}+s_{l,j}}{2}} \left(\eta^2 - \left(\frac{r_{l,j}-s_{l,j}}{2}\right)^2\right)^q \mathrm{d}\eta
\end{aligned}
\tag{16}
$$

Based on the equation for $\nu \neq 0$ [19]

$$
\int_0^\mu \left(x^2 - \nu^2\right)^p \mathrm{d}x = (-1)^p \mu \nu^{2p}{}_2\mathrm{F}_1\left(-p, \frac{1}{2}; \frac{3}{2}; \frac{\mu^2}{\nu^2}\right)
\tag{17}
$$

Equation (16) becomes

$$\int_{-\frac{r_{l,j}+s_{l,j}}{2}}^{1-\frac{r_{l,j}+s_{l,j}}{2}} \left(\eta^2 - \left(\frac{r_{l,j}-s_{l,j}}{2}\right)^2\right)^q d\eta$$

$$= (-1)^q \left(1 - \frac{r_{l,j}+s_{l,j}}{2}\right) \left(\frac{r_{l,j}-s_{l,j}}{2}\right)^{2q} {}_2F_1\left(-q, \frac{1}{2}; \frac{3}{2}; \frac{(2-r_{l,j}-s_{l,j})^2}{(r_{l,j}-s_{l,j})^2}\right) \qquad (18)$$

$$+ (-1)^q \left(\frac{r_{l,j}+s_{l,j}}{2}\right) \left(\frac{r_{l,j}-s_{l,j}}{2}\right)^{2q} {}_2F_1\left(-q, \frac{1}{2}; \frac{3}{2}; \frac{(r_{l,j}+s_{l,j})^2}{(r_{l,j}-s_{l,j})^2}\right)$$

where $_2F_1(a, b; c; z) = \frac{\Gamma(c)}{\Gamma(b)\Gamma(c-b)} \int_0^1 x^{b-1} (1-x)^{c-b-1} (1-zx)^{-a} dx$ is the Gaussian hypergeometric function and $(-1)^q$ refers to the single-valued analytic continuous branch of the principal value of the argument [18, 20].

To summarize, the closed-form expression of Equation (2) is

$$\sigma_{ISI}^2 = \frac{8}{2-\alpha}\pi^2 k^2 L A_K(\alpha) \hat{C}_n^2 \Gamma\left(\frac{4-\alpha}{2}\right) \sum_{j=1}^2 \sum_{l=1}^2 (-1)^{j+l} \Re\left\{\left(-\frac{z_l}{4}\left(r_{l,j}-s_{l,j}\right)^2\right)^q\right.$$

$$\times \left[\left(\frac{r_{l,j}+s_{l,j}}{2}\right)_2 {}_2F_1\left(-q, \frac{1}{2}; \frac{3}{2}; \frac{(r_{l,j}+s_{l,j})^2}{(r_{l,j}-s_{l,j})^2}\right)\right. \qquad (19)$$

$$\left.\left.+ \left(1 - \frac{r_{l,j}+s_{l,j}}{2}\right)_2 {}_2F_1\left(-q, \frac{1}{2}; \frac{3}{2}; \frac{(2-r_{l,j}-s_{l,j})^2}{(r_{l,j}-s_{l,j})^2}\right)\right]\right\}$$

Equation (19) is valid for $r_{l,j} \neq s_{l,j}$, otherwise it should be revised by Equation (15).

4 NUMERICAL SIMULATIONS

This section conducts numerical simulations to analyse the influences of α, l_0, L_0, ς_e and λ on the $\sigma_{ISI}^2(D_G)$ for different Gaussian beams. The simulations performed in this paper, however, should be only considered as arbitrary examples to indicate certain trend of results. Unless specified otherwise, all the numerical simulations are conducted with the default settings: $\alpha \in \{3, 4\}$, $C_n = 5.0 \times 10^{-15} m^{3-\alpha}$, $\varsigma_e = 1.5$, $l_0 = 0.01$m, $L_0 = 10$m, $\lambda = 1.55 \times 10^{-6}$m, $k \approx 4.05 \times 10^6$rad / m, $L = 4000$m, $\Lambda_0 = 0.1$, $\Theta_0 \in \{0.9, 1, 1.1\}$, $D_G = 0.15$m, $\Omega_G \approx 0.70 > \max \Lambda \approx 0.12$. Of course, other values which satisfy can also be chosen.

Figure 2 depicts $\sigma_{ISI}^2(D_G)$ for different Gaussian beams as a function of α for several pairs of $l_0 \in \{0.001, 0.01, 0.1\}$ and $L_0 \in \{1, 10, 100\}$. Figure 2 indicates that $\sigma_{ISI}^2(D_G)$ increases with a decrease in l_0 or an increase in L_0. These phenomena can be physically explained by the fact that l_0 and L_0 define the upper and lower bounds of the turbulent inertial subrange, respectively. As l_0 decreases or L_0 increases, the turbulent inertial subrange extends
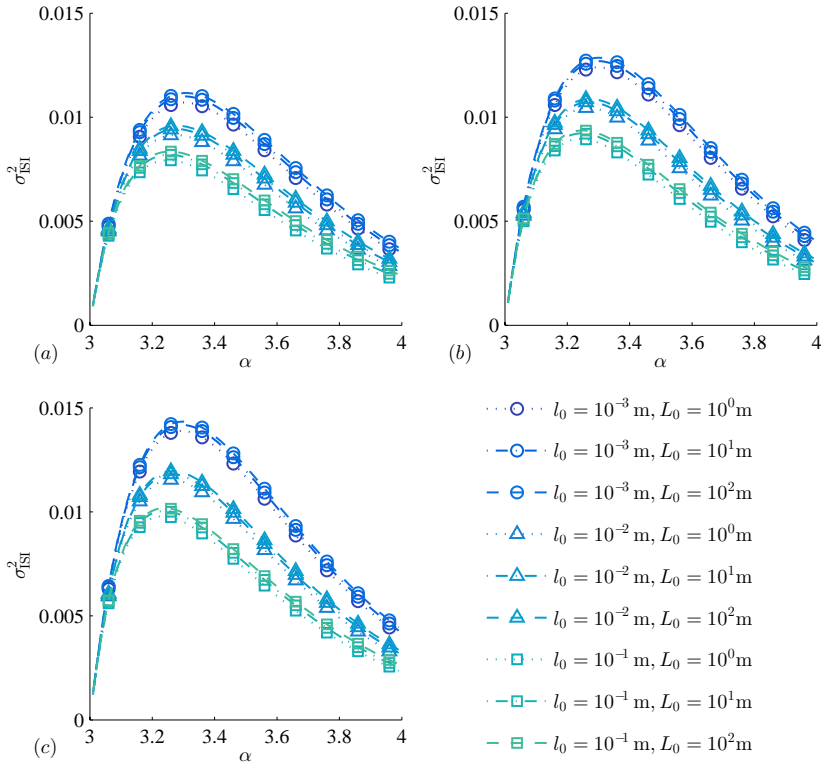
FIGURE 2

Graphs showing (a) convergent beam (Θ=0.9), (b) collimated beam (Θ_0=1.0) and (c) divergent beam (Θ_0=1.0) for $\sigma_{ISI}^2 (D_G)$ of different Gaussian beams as a function of α for several pairs of l_0 and L_0.

and the Gaussian beam will meet more turbulent eddies along its propagation. Thus, the turbulence effects strengthen and $\sigma_{ISI}^2 (D_G)$ increases. Figure 2 also indicates that $\sigma_{ISI}^2 (D_G)$ is more sensitive to the change of l_0 than L_0, which implies that $\sigma_{ISI}^2 (D_G)$ is related to those small-scale turbulent eddies. Besides, as shown in Figure 2, $\sigma_{ISI}^2 (D_G)$ first increases and then decreases with an increase in α when other parameters are fixed. Mathematically, according to Figure 1, $A(\alpha)$ increases monotonically from $\lim\limits_{\alpha \to 3} A(\alpha) = 0$ and dominates the calculation of $\sigma_{ISI}^2 (D_G)$, whereas when $3.3 < \alpha < 4$ the term $\exp\left(-\frac{\varsigma_e^2 \kappa^2}{\kappa_H^2}\right)$ takes over, which can be regarded as a low-pass filter about κ. As mentioned above, κ_H decreases with an increase in α; that is, larger α allows less turbulence cells to contribute to $\sigma_{ISI}^2 (D_G)$.

Figure 3 depicts $\sigma_{ISI}^2 (D_G)$ for different Gaussian beams as a function of α for several pairs of $\varsigma_e \in \{1, 1.5, 2\}$ and $\lambda \in \{0.85 \times 10^{-6}, 1.06 \times 10^{-6}, 1.55 \times 10^{-6}\}$, where $\min \Omega_G \approx 0.22 > \max \Lambda \approx 0.12$. Figure 3 indicates
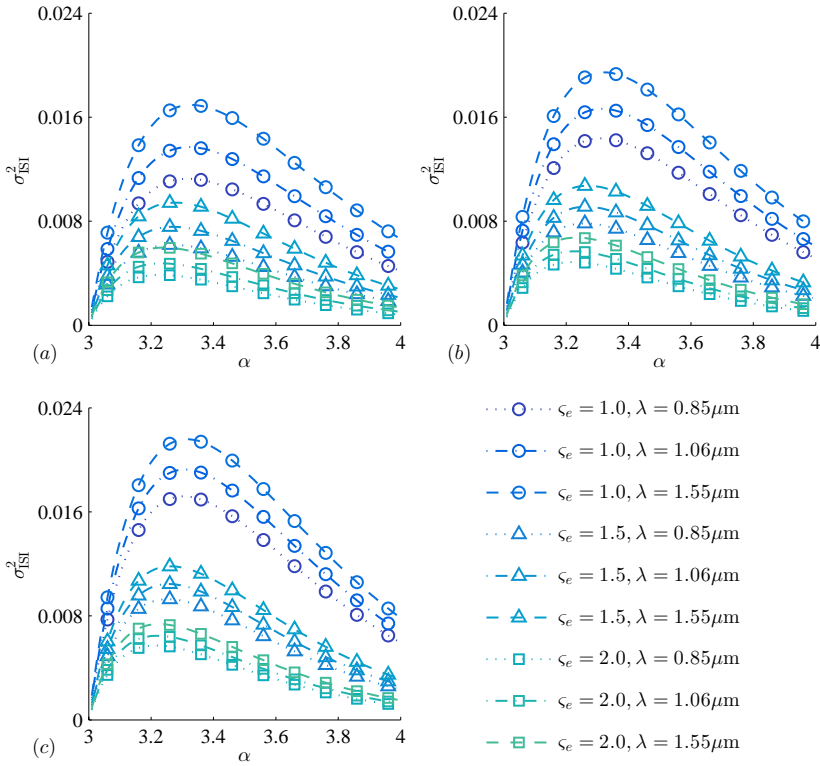
FIGURE 3

Graphs showing (a) convergent beam ($\Theta = 0.9$), (b) collimated beam ($\Theta_0 = 1.0$) and (c) divergent beam ($\Theta_0 = 1.0$) for $\sigma_{ISI}^2 (D_G)$ of different Gaussian beams as a function of α for several pairs of ς_e and λ.

that $\sigma_{ISI}^2 (D_G)$ decreases with an increase in ς_e. Physically, this phenomenon is caused by stochastic fluctuations of curvature among the anisotropic turbulence cells. Acting as lenses with large radii of curvature, these anisotropic turbulence cells can significantly modify the focusing properties of the transmission media. The larger radius of curvature, which means an increasing anisotropic factor mathematically, makes the optical beam less deviated from its propagation path. Ultimately, $\sigma_{ISI}^2 (D_G)$ will take smaller value. Figure 3 also indicates that $\sigma_{ISI}^2 (D_G)$ decreases with an increase in λ. This phenomenon may be caused by the fact that the longer the beam wavelength, the more pronounced is the diffraction. Thus, a laser beam with longer wavelength can be less affected by small-scale turbulent eddies.

Figure 4 depicts $\sigma_{ISI}^2 (D_G)$ for different Gaussian beams as a function of α for several pairs of $L \in \{3000, 4000, 5000\}$ and $D_G \in \{0.1, 0.15, 0.2\}$, where $\min \Omega_G \approx 0.30 > \max \Lambda \approx 0.12$. Figure 4 indicates that $\sigma_{ISI}^2 (D_G)$ decreases with an increase in D_G when other parameters are fixed. It is known
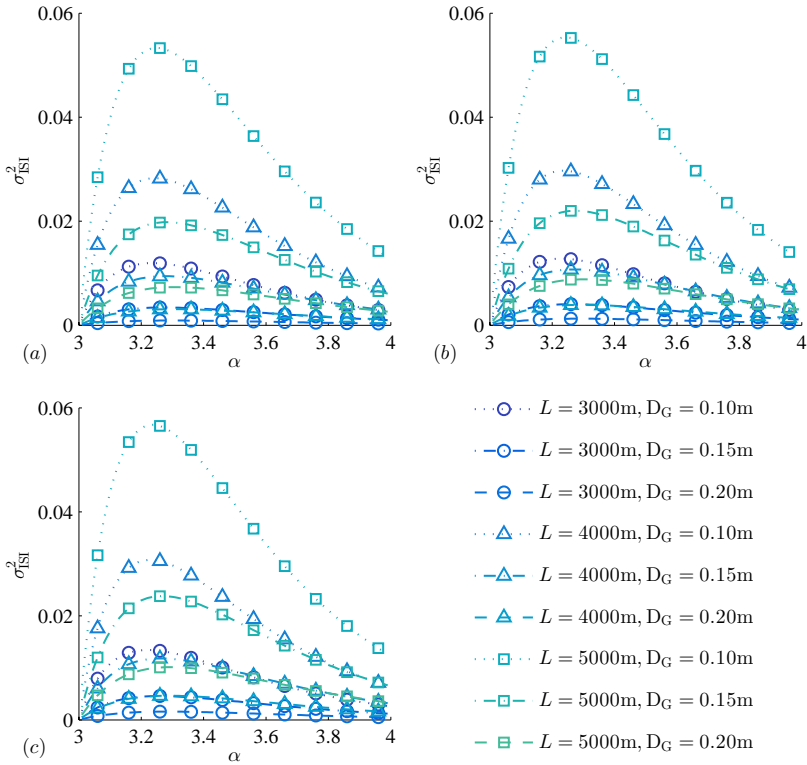
FIGURE 4

Graphs showing (a) convergent beam ($\Theta = 0.9$), (b) collimated beam ($\Theta_0 = 1.0$) and (c) divergent beam ($\Theta_0 = 1.0$) for $\sigma^2_{ISI}(D_G)$ of different Gaussian beams as a function of α for several pairs of L and D_G.

that the irradiance scintillation under weak fluctuation, regarded as the synthesis of forward scattering cells, is a second central moment after regularization. A lager D_G means more forward scattering cells. According to the law of large numbers and the central limit theorem, if these forward scattering cells are independent and identically distributed random variables, their second central moment decreases with an increase in the number of samples, and thus $\sigma^2_{ISI}(D_G)$ decreases.

5 CONCLUSIONS

The aperture-averaged irradiance scintillation derived for a Gaussian beam propagating through the weak anisotropic atmospheric turbulence along a horizontal path has been investigated. The generalized exponential spectrum is utilized to take the variable spectral power law value, finite inner and

outer scales of turbulence, the anisotropic factor, and other important optical parameters of a Gaussian beam into account. The analytical expressions are deduced by complex analysis. The simulation results show that the aperture-averaged irradiance scintillation index (ISI) will:

(i)   Decrease with an increase in the inner scale or the anisotropic factor or the wavelength or the collecting lens diameter;
(ii) Decrease with a decrease in the outer scale or the propagation path length;
(iii) First increase and then decrease with an increase in the spectral power law; and
(iv) Be more sensitive to the inner scale than the outer scale.

NOMENCLATURE

$A(\alpha)$	Function of α
$C(\alpha)$	Function of α
C_n	Generalized atmospheric structure parameter ($\mathrm{m}^{3-\alpha}$)
d_1	Parameter of $f(\kappa)$
d_2	Parameter of $f(\kappa)$
D_G	Collecting lens diameter (m)
$f(\kappa)$	Function of κ
$_2F_1(.;.;.;)$	Gaussian hypergeometric function
$G_{l,j}(\xi)$	Univariate quadratic polynomials about ξ
k	Angular wavenumber of the Gaussian wave (rad/m)
L	Length along the propagation path (m)
l_0	Inner scale of turbulence (m)
L	Outer scale of turbulence (m)
$P(\xi)$	Function of ξ
q	Constant related to α
$Q(\xi)$	Function of ξ
$r_{l,j}$	Root of $G_{l,j}(\xi)= 0$
R_0	Phase front radius of the Gaussian wave at transmitter (m)
$s_{l,j}$	Root of $G_{l,j}(\xi)= 0$
w_0	Waist radius (m)
W_0	Waist size of the Gaussian wave (m)
z	Coordinate along the propagation direction (m)
z_1	Coefficient of $G_{l,j}(\xi)$
z_2	Coefficient of $G_{l,j}(\xi)$

Greek symbols

α	Spectral power law value
$\Gamma(.)$	Gamma function
Θ	Refraction parameter of the Gaussian wave at the receiver

Θ_0	Curvature parameter of the Gaussian wave at the transmitter
$\overline{\Theta}$	Complementary parameter of the Gaussian wave at the receiver
κ	Angular wavenumber (rad/m)
κ_H	Constant value related to the inner scale of turbulence (rad/m)
κ_L	Constant value related to the outer scale of turbulence (rad/m)
κ_x	Component of the angular wavenumber of turbulence in the $x-$direction (rad/m)
κ_y	Component of the angular wavenumber of turbulence in the $y-$direction (rad/m)
κ_z	Component of the angular wavenumber of turbulence in the $z-$direction (rad/m)
Λ	Optical parameter of the Gaussian wave at the receiver
Λ	Fresnel ratio of the Gaussian wave at the transmitter
Λ	Wavelength of the Gaussian beam (m)
ξ	Normalized path coordinate
σ_{ISI}^2	Aperture-averaged ISI of a Gaussian wave
ς_e	Anisotropic factor
$\Phi_n(.)$	Generalized exponential spectrum for anisotropic turbulence
Ω_G	Non-dimensional parameter characterizing the relative radius of the collecting lens

Mathematical operators

$\Re$	Real part of a complex number

REFERENCES

[1] Andrews L.C. and Phillips R.L. *Laser Beam Propagation Through Random Media.* Bellingham: SPIE Press 2005.

[2] Gao C. and Li X. Effects of inner and outer scale on the modulation transfer function for a Gaussian beam propagating through anisotropic non-Kolmogorov turbulence. *Optical Review* **24**(3) (2017), 253–259.

[3] Mansour A., Mesleh R. and Abaza M. New challenges in wireless and free space optical communications. *Optics and Lasers in Engineering* **89**(1) (2017), 95–108.

[4] Kaushal H. and Kaddoum G. Optical communication in space: challenges and mitigation techniques. *IEEE Communications Surveys and Tutorials* **19**(1) (2017), 57–96.

[5] Li Y., Gao C., Liang H., Miao M. and Li X Performance of an adaptive phase estimator for coherent free-space optical communications over Gamma-Gamma turbulence. *Optics Communications* **388**(1) (2017), 47–52.

[6] Cui L. Irradiance scintillation index for Gaussian beam based on the generalized anisotropic von Karman spectrum. *Infrared Physics and Technology* **77**(1) (2016), 431–439.

[7] Cui L. Irradiance scintillation of Gaussian beam considering the concept of anisotropy at different scales in weak anisotropic turbulence. *Optik* **127**(20) (2016), 9328–9337.

[8] Cui L. and Cao L. Irradiance scintillation considering finite turbulence inner scale for optical wave propagating through weak non-Kolmogorov turbulence. *Optik* **124**(24) (2013), 6684–6689.

[9] Cui L., Xue B., Xue W., Bai X., Cao X. and Zhou F. Expressions of the scintillation index for optical waves propagating through weak non-Kolmogorov turbulence based on the generalized atmospheric spectral model. *Optics & Laser Technology* **44**(1) (2012), 2453–2458.

[10] Cui L., Xue B., Cao L., Zheng S., Xue W., Bai X., Cao X. and Zhou F. Irradiance scintillation for Gaussian-beam wave propagating through weak non-Kolmogorov turbulence. *Optics Express* **19**(18) (2011), 16872–16884.

[11] Toselli I., Agrawal B. and Restaino S. Light propagation through anisotropic turbulence. *Journal of the Optical Society of America A: Optics, Image Science and Vision* **28**(3) (2011), 483–488.

[12] Tan L., Du W., Ma J., Yu S. and Han Q. Log-amplitude variance for a Gaussian-beam wave propagating through non-Kolmogorov turbulence. *Optics Express* **18**(2) (2010), 451–462.

[13] Toselli T., Andrews L., Phillips R. and Ferrero V. Free space optical system performance for a Gaussian beam propagating through non-Kolmogorov weak turbulence. *IEEE Transactions on Antennas and Propagation* **57**(6) (2009), 1783–1788.

[14] Toselli I. and Korotkova O. General scale-dependent anisotropic turbulence and its impact on free space optical communication system performance. *Journal of the Optical Society of America A: Optics, Image Science and Vision* **32**(6) (2015), 1017–1025.

[15] Cheng M., Guo L. and Zhang Y. Scintillation and aperture averaging for Gaussian beams through non-Kolmogorov maritime atmospheric turbulence channels. *Optics Express* **23**(25) (2015), 32606–32621.

[16] Gao C., Li Y., Li Y. and Li X. Irradiance scintillation index for a Gaussian beam based on the generalized modified atmospheric spectrum with aperture averaged. *International Journal of Optics* **2016**(1) (2016), 8730609.

[17] Gao C. and Li X. Effects of inner and outer scale on beam spreading for a Gaussian wave propagating through anisotropic non-Kolmogorov turbulence. *Optica Applicata* **47**(1) (2017), 63–74.

[18] Olver F. W. J., Lozier D. W., Boisvert R. F. and Clark C. W. *NIST Handbook of Mathematical Functions*. London: Cambridge University Press. 2010.

[19] Gradshteyn I. S. and Ryzhik, I. M. *Table of Integrals, Series, and Products*. New York: Academic Press 2014.

[20] Zwillinger D *CRC Standard Mathematical Tables and Formulae*. Boca Raton: CRC Press 2011.